A Simple Graphical Procedure for Determining Cyclic Elasto-Plastic Notch Stresses

JOHN M. POTTER
Air Force Flight Dynamics Laboratory, Dayton, Ohio

A new combination of the Neuber elasto-plastic notch relation and material property data is proposed and investigated for a general graphical analysis of local stresses during cyclic loading. The technique is applied to 2024-T4 aluminum alloy. The resulting stress analysis is shown to accurately reflect local stress levels at notches by comparison with measured local stress levels. Life to failure predictions based on the graphically derived local stress levels compare favorably with constant stress amplitude notched coupon results. Applications of the graphical method to spectrum loading to demonstrate quantitative fatigue life effects of overloading and ground-air-ground cycles are discussed.

Nomenclature

E = modulus of elasticity
S = nominal stress
e = nominal strain
K_T = elastic stress concentration factor
K_σ = actual local stress concentration factor
K_ε = actual local strain concentration factor
K_f = fatigue strength reduction factor
$K_T S$ = notch stress
R = stress ratio, S_{min}/S_{max}
N_f = cycles to failure
σ = local stress at notch or unnotched coupon stress level
ε = local strain at notch or unnotched coupon strain level
$\Delta S, \Delta e$ = change in nominal or local stress or strain levels from $\Delta\sigma, \Delta\varepsilon$ reversal-to-reversal
σ_R = zero load local stress level (residual stress)
i = reversal number, 1, 2, 3 . . .

Introduction

SEVERAL investigators[1-5] have shown the Neuber[6] elasto-plastic analysis to be a reasonable model for relating stresses in the neighborhood of a notch to the nominal stresses. Much of this work involved determining experimental analogs for specific load sequences or conditions. These investigators have shown that a successful fatigue life correlation to notched coupons can be obtained by testing unnotched coupons to repeated cyclic loading between stress and strain limits determined from the Neuber analysis. The simplicity and elementary nature of the technique, along with the apparent success in correlating fatigue lives, gives one hope that the Neuber analysis may help remove the uncertainties seen with fatigue design and analysis during spectrum loading along with the expensive results of unrealistic predictions.

Unfortunately, the average designer does not have a test machine available to him to aid in determining residual stresses and their effect on the fatigue life of a potential design. Potter[7] utilized the principles of the Neuber analysis to develop a simple, graphical, design-oriented method for calculating local stresses during cyclic loading. He used published elasto-plastic properties for two common aircraft materials and made good fatigue life predictions of notched coupons from knowing only the developed local stress analysis and handbook S-N data on unnotched coupons. The objective of this paper is to refine the graphical local stress analysis and to discuss its potential usage in aircraft fatigue design and operation. This local stress analysis is intended both as an aid to the understanding of residual stresses and for quantitatively and qualitatively determining the effect of these stresses on a spectrum fatigue life.

Stress Analysis at Notches

Because fatigue failures invariably start at stress concentrations, the stress state at the notch is significant to fatigue and fatigue predictions. To implement residual stress modified fatigue analysis, one must first be able to determine the residual stresses.

For many structures, service loads will induce localized plastic deformation around stress concentrations. With notch plasticity there is a local permanent set or redistribution of displacements. Upon subsequent unloading, the material surrounding the plastically deformed region attempts to force the affected portion to return to its original shape, thus causing what are called residual stresses. These residual stresses alter the local stress state by adding or subtracting from the elastically calculated notch stresses. The local stress following localized plastic deformation is determined by the equation

$$\sigma = K_T S + \sigma_R \tag{1}$$

According to Neuber[6] the local stresses and strains are related to the nominal stresses by the equation

$$K_T^2 = K_\sigma K_\varepsilon \tag{2}$$

Replacement of K_σ and K_ε with their stress and strain equivalents gives the relation

$$K_T^2 = (\sigma/S)(\varepsilon/e) \tag{3}$$

If there is no gross yielding of the section, the nominal strain is elastically proportional to the nominal stress and Eq. (3) can be rewritten as

$$(K_T S)^2/E = \sigma\varepsilon \tag{4}$$

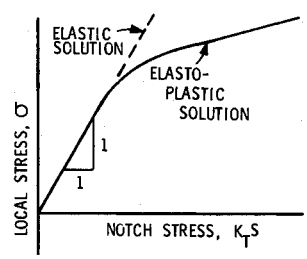

Fig. 1 Local stress as a function of notch stress.

Received July 6, 1971; presented as Paper 71-776 at the AIAA 3rd Aircraft Design and Operations Meeting, Seattle, Wash., July 12–14, 1971; revision received April 3, 1972. This work has been accomplished in the Experimental Branch, Structures Division of the Air Force Flight Dynamics Laboratory. The author wishes to acknowledge the efforts of J. N. Marable and W. J. Shiner for their assistance in the setup and operation of the hybrid computer control system. He particularly wishes to thank R. L. Cavanagh and S. Lustig for their continuing support and encouragement.

Index category: Aircraft Structural Design (Including Loads).

* Captain, U.S. Air Force, Astronautical Engineer.

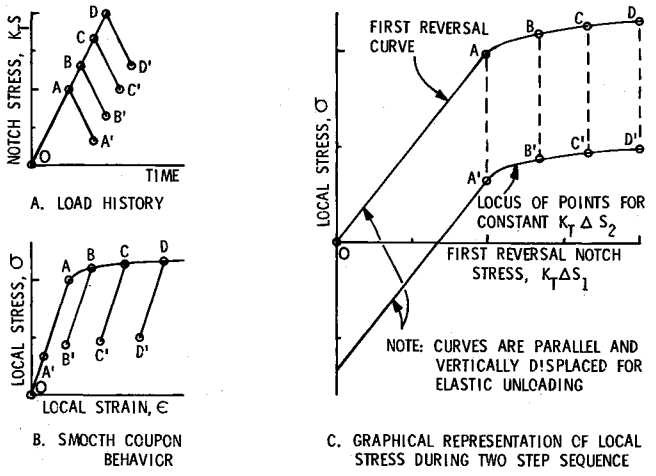

Fig. 2 Development of a local stress analysis for a two step nominal stress sequence.

As K_TS increases from zero, unique values of local stress and strain exist that satisfy this relation. Utilizing stress-strain data from smooth specimens, localized stresses at notches can be obtained by solving Eq. (4) directly for stress for any material of interest. Figure 1 schematically illustrates a local stress vs notch stress curve for monotonic loading. The corresponding local strain vs notch stress curve could also be constructed.

To allow for fatigue loading the Neuber relation [Eq. (4)] would be used with peak-to-peak load changes to obtain continuing local stress values. For this case the stress (S and σ) and strain (ε) terms in Eq. (4) are replaced with change in stress and strain terms on a reversal-to-reversal basis using

$$(K_T\Delta S_i)^2/E = \Delta\sigma_i\,\Delta\varepsilon_i \tag{5}$$

A single curve representation of sequence effects is obtained by changing the notch stress (K_TS) axis in Fig. 1 to a first reversal notch stress ($K_T\Delta S_1$) axis. Figure 2 illustrates the procedure for developing a graphical local stress-notch stress relation for any general two step load sequence. Figure 2a shows the four load-unload sequences that are to be considered.

For the load-unload sequence *O-A-A'*, the local stress solution is calculable directly from the elastic notch analysis since no plastic flow has occurred. The local stress for this loading sequence is the calculated notch stress, K_TS.

For the loading sequences *O-B*, *O-C*, and *O-D*, plastic deformation occurs at the notch so that, during any subsequent unloading from load levels *B*, *C*, and *D*, the local stress will depend upon this preceding maximum load. The local stress for the load position *B'* is determined knowing the local stress for position *B* and using the modified Neuber equation, [Eq. (5)] applied to the unloading behavior of unnotched coupons. A major simplicity is found during the initial portion of the unloading; conventional unnotched coupon materials testing shows that following each load reversal, the load-deformation response is initially elastic. When the unloading is locally elastic Eq. (5) reduces to

$$\Delta\sigma_i = K_T\Delta S_i \tag{5a}$$

Therefore, during the initial unloading the change in local stress is equal to the change in notch stress. In this case, for locally elastic material behavior during unloading, the local stress for load position *B'* is found from

$$\sigma_{B'} = \sigma_B + K_T\Delta S_{B-B'} \tag{6}$$

(The $\Delta S_{B-B'}$ for this unloading is negative.) Position *B'* is plotted directly below point *B* on the first reversal curve in Fig. 2c and is separated from point *B* by $K_T\Delta S_{B-B'}$. A similar procedure can be followed to determine the values of the local stress in sequences *O-C-C'* and *O-D-D'*. As Fig. 2c indicates, the locus of local stress levels, following an arbitrary initial loading of $K_T\Delta S_1$ and elastic unloading of $K_T\Delta S_2$, is a curve that is vertically displaced from the first reversal curve by an amount $K_T\Delta S_2$. Note that it is necessary to associate both initial loading and the following unloading history to determine the local stress after unloading.

Similar curves for other values of $K_T\Delta S_2$ can be drawn which are parallel and vertically displaced ad infinitum from the first reversal curve were it not for yielding in compression. When yielding occurs in compression upon unloading, the local stress values are determined using the generalized Neuber relation [Eq. (5)] in conjunction with unnotched coupon stress-strain behavior. For a constant $K_T\Delta S_2$, compressive yielding is experienced first at the lower values of $K_T\Delta S_1$. Thus, the curves for a constant $K_T\Delta S_2$, which are exact images of the first reversal curve for elastic unloading, become "*S*" shaped and finally almost flat as $K_T\Delta S_2$ increases.

The zero load local stress level (residual stress) following a load-unload sequence is dependent on the maximum notch stress. The residual stress is the local stress for a $K_T\Delta S_2 = -K_T\Delta S_1$. Thus, the residual stress subsequent to a $K_T\Delta S_1 = 100$ ksi load would be found at the intersection of the abscissa value of 100 ksi and the $K_T\Delta S_2 = -100$ ksi curve.

The choice of the stress-strain relation to be used in this analysis is dependent on the specific situation to be analyzed. One could use either the monotonic or the cyclic stress-strain relation. The cyclic stress-strain curve may possibly be used when many cycles of fully reversed high-amplitude loading are expected on the notched component. When the loading is essentially unidirectional and when few excursions of notch stress above the monotonic yield strength are expected, it is more reasonable to use the monotonic stress-strain relation. Since this author is primarily interested in aircraft structures where the loads are closer to the second case than the first, the monotonic stress-strain relation was investigated.

Development of Local Stress Analysis

A common aircraft aluminum alloy, 2024-T4, was chosen for the experimental determination of the $K_T\Delta S_1$-vs-σ curve. Seven specimens were loaded to determine this curve which is shown in Fig. 3. The specimens represented $K_T\Delta S_1$ values of 5, 30, 60, 80, 100, 120, and 160 ksi. Table 1 shows the pertinent data derived for each specimen. The specimens were tested in a closed loop hydraulic test frame with a digital computer feedback control and readout system. The first reversal was chosen to be of positive or tensile load. The specimens were incrementally strain controlled until the desired first reversal product of local stress and strain was reached. At this point, the control signal was reversed and the strain incrementally decreased until the test was stopped due to gross specimen buckling. Stress, strain, the product of stress and strain, and the associated $K_T\Delta S$ were calculated and

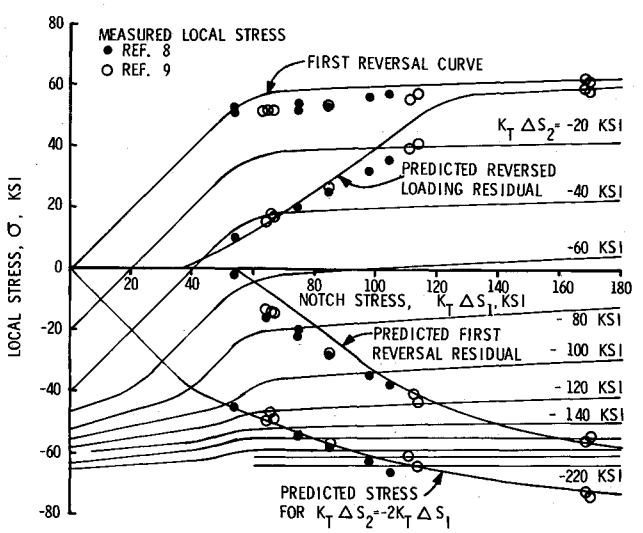

Fig. 3 Empirically derived $K_T\Delta S_1$-vs-σ curve for 2024-T4 with comparison to measured local stress levels.

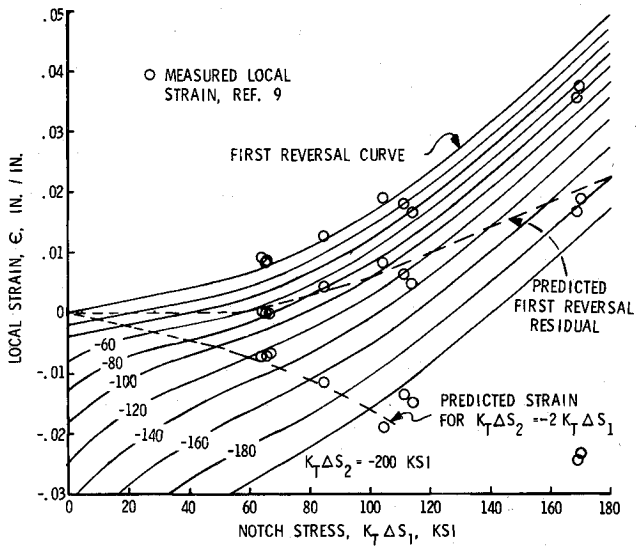

Fig. 4 Empirically derived $K_T\Delta S_1$-vs-ε curve for 2024-T4 with comparison to measured local strain levels.

stored for each increment during the loading cycle. The controlled strain increments were approximately 90 μ *in*/in. These data were printed out in digital form for detailed analysis. Strain was measured with a 1-in. gage length clip gage extensometer.

Figure 3 shows the resultant $K_T\Delta S_1$-vs-σ curve. Superimposed on the curve are measured local stress values from Crews[8,9] for 2024-T3 and the corresponding local stress prediction during reversed loading according to the analysis outlined in the previous section. The correlation of local stress is very good. Crews' data were obtained on panels with K_T values of 2, 4, and 6 illustrating the generality of the analysis.

The residual stress prediction for zero load, following completely reversed loading, assumes initially elastic unloading from the compressive peak and monotonic tensile yield behavior above a local stress of zero. This assumption ignores the commonly seen Bauschinger effect of a reduced yield stress following plastic flow in the opposite direction. A study of the Bauschinger effect for all possible cases of loading sequences was beyond the scope of this effort. Since this specific analysis is aimed toward aircraft structural application where considerable amounts of cyclic plasticity are not present, the lack of sophistication in accounting for this effect is not significant.

There is, of course, a local strain associated with the local stress. A figure similar to the $K_T\Delta S_1$-vs-σ curve can be drawn and the same sort of data comparison done as a check on the Neuber relation. Figure 4 shows such a curve with Crews' data superimposed on it. Again the measured data show good correlation with that predicted from the unnotched specimens tested in accordance with the Neuber relation.

The main discrepancy between the measured local stress and strain behavior and the unnotched coupon Neuber modeled local prediction seems to come from a tensile yield stress difference. Crews' data were from 2024-T3 material with a yield stress of 52 ksi, while the $K_T\Delta S_1$ analysis was based on a 58 ksi yield material.

Fatigue Analysis Technique

With the stress analysis derived in the previous section, one can determine local stress amplitudes and mean stresses for cyclic nominal stress loading. The calculation of local stress level and fatigue life in constant amplitude loading is done as follows. 1) Determine notched specimen $K_T\Delta S_1$; find σ_{max} on "first reversal curve" of $K_T\Delta S_1$-vs-σ curve. This is the σ_{max} value. 2) Determine $K_T\Delta S_2$ value from constant amplitude nominal stress history. Go to $K_T\Delta S_1$-vs-σ curve at $K_T\Delta S_1, \sigma_{max}$ position. Drop vertically until the required $K_T\Delta S_2$ is reached. This is the σ_{min}. 3) These values of σ_{max} and σ_{min} are the local stress values during the constant amplitude loading of notched coupons. Fatigue life of the notched coupon is the estimated by determining the fatigue life for unnotched coupons between $\sigma_{max} - \sigma_{min}$ constant amplitude.

Thus, knowing the geometry of the specimen (i.e., K_T) and the testing conditions (R, S_{max}, S_{mean}, etc.), a fatigue life prediction can be made based on the stress level at the notch found in the $K_T\Delta S_1$-vs-σ curve. For example, assume 2024-T4 material notched to $K_T = 2.0$ and tested at $R = 0$ with $S_{max} = 40{,}000$ psi. From Fig. 3 at $K_T\Delta S_1 = 80{,}000$, σ_{max} is found to be 57 ksi. Dropping vertically be $K_T\Delta S_2 = 80{,}000$ gives $\sigma_{min} = -21$ ksi. The local stress level during cycling would be described as -21 ksi

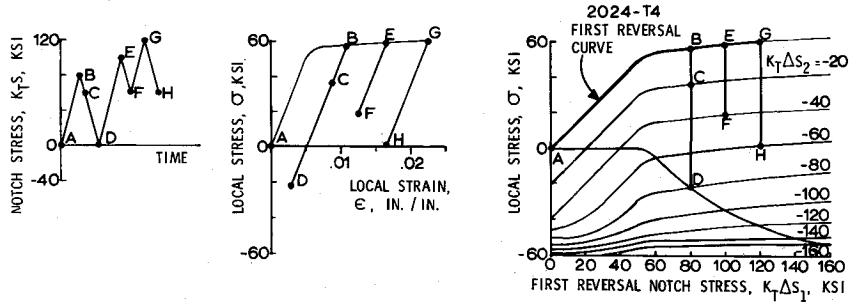

A. CASE I LOCAL STRESS ANALYSIS FOR LITTLE OR NO CYCLIC PLASTICITY

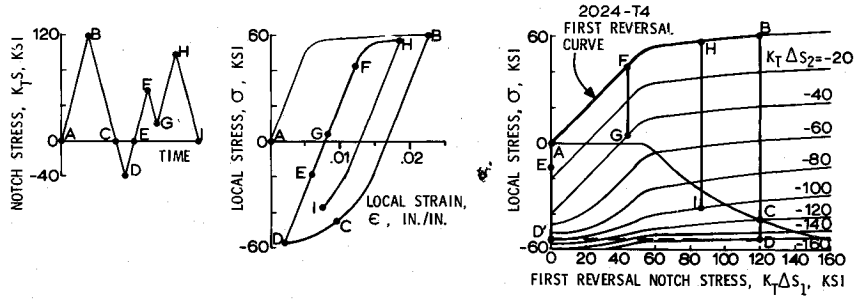

B. CASE II LOCAL STRESS ANALYSIS FOR OCCASIONAL CYCLIC PLASTICITY
(THIS LOCAL STRESS ANALYSIS IS NOT APPLICABLE FOR CYCLIC LARGE AMPLITUDE FULLY REVERSED LOADING)

Fig. 5 Examples of local stress level tracking for spectrum loading using the $K_T\Delta S_1$-vs-σ analysis.

Table 1 Measured local stress and strain values to determine the $K_T\Delta S_1$-vs-σ and -ε relations for 2024-T4 aluminum alloy

$K_T\Delta S_1$, ksi	σ, ksi ε, (in./in.) at $K_T\Delta S_1$	σ, ksi ε, in./in. at $K_T\Delta S_2$									
		−20	−40	−60	−80	−100	−120	−140	−160	−180	−200
5	5.1	−16.5	−34.7	−45.0	−50.5	−54.2	−57.1	−59.7	−62.4	−65.1	...
	0.0004	−0.0016	−0.0036	−0.0067	−0.0108	−0.0161	−0.0222	−0.0290	−0.0364	−0.0447	...
30	30.1	9.8	−10.2	−30.9	−43.4	−49.1	−53.8	−56.9	−59.9	−63.1	−65.9
	0.0028	0.0009	−0.0009	−0.0030	−0.0055	−0.0087	−0.0137	−0.0189	−0.0245	−0.0307	−0.0372
60	55.2	34.2	15.1	−5.2	−24.5	−39.7	−47.6	−51.9	−54.9	−57.8	−60.8
	0.0063	0.0044	0.0025	0.0005	−0.0015	−0.0038	−0.0073	−0.0114	−0.0162	−0.0216	−0.0280
80	57.1	36.1	17.2	−2.4	−21.4	−36.9	−46.8	−51.8	−55.3	−58.1	−60.7
	0.0109	0.0088	0.0069	0.0049	0.0028	0.0004	−0.0028	−0.0067	−0.0114	−0.0166	−0.0221
100	59.6	40.0	20.5	0.3	−17.6	−33.7	−45.0	−51.8	−55.8	−58.8	−61.1
	0.0163	0.0144	0.0123	0.0102	0.0081	0.0057	0.0029	−0.0009	−0.0053	−0.0104	−0.0159
120	61.5	41.6	20.9	1.6	−16.6	−33.4	−45.1	−52.4	−56.8	−60.0	−62.1
	0.0228	0.0209	0.0189	0.0169	0.0148	0.0124	0.0096	0.0060	0.0018	−0.0033	−0.0086
160	63.1	42.6	24.4	5.8	−11.7	−28.1	−40.8	−49.8	−55.3	−58.8	−61.5
	0.0399	0.0377	0.0356	0.0336	0.0313	0.0290	0.0263	0.0229	0.0187	0.0139	0.0086

to +57 ksi, compared to the elastic assumption of local stress of 0 to 80 ksi. Fatigue life prediction in constant ΔS amplitude loading is then determined from the Modified Goodman Diagram of unnotched axial loaded specimens of the desired material. Unnotched S-N-data[10] indicate a life of 10,000 cycles for this condition.

The prediction of local stress levels during spectrum loading is somewhat more complicated but can be accomplished in a straightforward manner using the graphical technique of Fig. 3. In spectrum loading there are three cases to be considered that can be generally differentiated by the amounts of cyclic plasticity involved.

1. Little or No Cyclic Plasticity

This case is usually limited to unidirectional loading. Figure 5a illustrates this case for an increasing peak load. In a succession of peak loads as in points B, E, and G the effective $K_T\Delta S_1$ increases and remains equal to the current K_TS_{peak}. For successive cycles where the peak is less than the previous maximum, the local stress levels would be adequately determined by Eq. (1) using the appropriate residual stress level, assuming a stable residual stress. It is interesting to note the changing local stress levels at constant notch stresses for the sequential points C, F, and H. The stress-strain behavior seen in Fig. 5 is derived from the data in Table 1 and is for 2024-T4 material.

2. Occasional Cyclic Plasticity

This case, illustrated in Fig. 5b, is characterized by unidirectional loading with occasional small compressive loads. For the unidirectional loading portion, the analysis is the same as that just described. During the compressive peak, point D, the local minimum stress level is determined in the usual manner for the second reversal. For subsequent reversals one assumes that the initial unloading stress-strain behavior is elastic. This author finds it convenient to further assume that the tensile stress-strain response does not change significantly during the analysis. Therefore, following the compressive peak, the effective $K_T\Delta S_1$ level, D', is re-established at zero, keeping the value of the second reversal local stress, and the analysis continued for the following reversals.

This case has application to the study of the effects of the ground-air-ground cycle in aircraft wing structures. The effect of the G-A-G cycle on local behavior is illustrated in the sequence A-E in Fig. 5b. Following peak load B the residual stress is given by point C. The introduction of the compressive peak D causes the subsequent zero load residual stress to become that of point E, with a decrease in the beneficial residual stress because of the compressive yielding. A more compressive peak stress would have caused the residual stress to become even less beneficial and perhaps become positive. One must have another peak tensile load such as peak H to make the residual stress become more beneficial again.

3. Large Amplitude Fully Reversed Loading.

In this case, one can quickly become lost in the graphical analysis. Whether or not the material is stable or cyclically hardens or softens, this analysis has little application. It may be possible to construct a similar analysis form using the cyclic stress-strain relation to solve this situation although that has not been attempted in this program.

Correlation with Notched Coupon Results

Figures 6 and 7 show a comparison of the crack initiation life estimate described in this paper and constant amplitude notched coupon results. The numbers of cycles of life to complete coupon fracture are plotted since these data are more frequently obtained than life to crack initiation. Represented are K_T values of 2.0, 2.4, and 4.0 from several investigators.[1,11,12] The data include 2024-T3 material as well as 2024-T4, but it was assumed that the fatigue properties were identical. There is good correlation between the life estimation technique and the data. The prediction of life to crack initiation is seen to be almost uniformly conservative. This phenomenon would be intuitively expected upon reflection of the finite number of cycles necessary to cause a "small" crack to grow large enough to reach critical size. Note that this technique is able to correctly anticipate the upturn in the fatigue life curve at less than 10^5 cycles. This upturn results from tensile yielding at the notch causing compressive residual stresses.

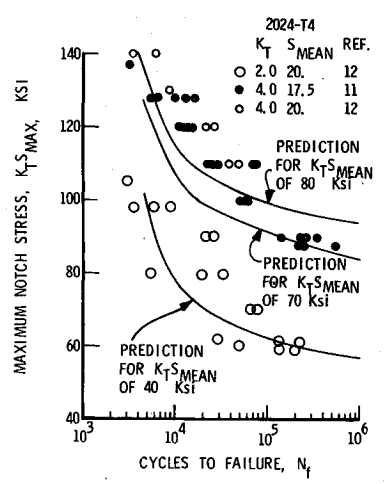

Fig. 6 Fatigue data vs predicted crack initiation life for 2024-T4 at three mean stresse.

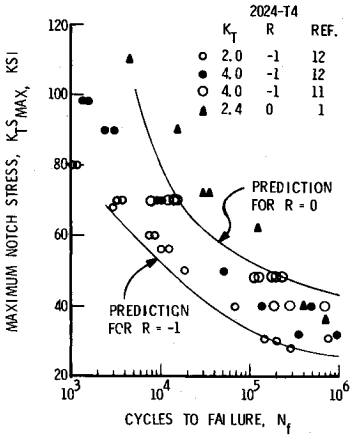

Fig. 7 Fatigue data vs predicted crack initiation life for 2024-T4 at stress ratios of −1 and 0.

Conventional elastic fatigue life predictions of constant amplitude notched coupon results from unnotched *S-N* data are seen to fit in the high cycle range, but are usually much too conservative in the 10^3 to 10^5 cycle range.

This author chooses not to correlate the observed fatigue behavior with unnotched coupon data through the quantity K_f, the fatigue strength reduction factor. In constant amplitude type loading the fatigue strength reduction factor is defined as the ratio of the stress for unnotched material to the nominal stress for notched material at the same fatigue life. The unnotched stress levels used to define K_f are almost invariably directly proportional to the elastic solution. So defined, K_f varies considerably as a function of the fatigue life,[13,14] and so its usefulness as a general design tool is debatable. Unless the local stress behavior is more accurately characterized by analyses such as that presented herein, it seems questionable to dwell on the potential of this quantity.

Discussion

The fact that this technique gives a good estimate of constant amplitude loaded fatigue lifetimes for notched coupons from a minimum of unnotched data is of little consequence in itself. Were it important to obtain the same data one could as easily cyclically load a series of notched coupons to obtain a general *S-N* curve for each design. But, upon further testing, designers usually find that spectrum load results are not well estimated from an elastic analysis done with the constant amplitude *S-N* data, even on the same design of component. Furthermore, minor changes in the spectrum or truncation of the high- or low-level cycles can cause drastic changes in the fatigue life. Surprisingly, eliminating the highest level cycles of a spectrum often shortens a notched structures lifetime[15] contrary to intuitive reasoning based on elastic analysis. In elastic analysis, using constant amplitude notched coupon data, one would assume that all tensile loads are damaging and that compressive loads do a minimal amount of damage; but, it has been found that the load reversals into compression on aircraft (e.g., ground-air-ground cycles) can be a major contributor of fatigue damage.[16] All these phenomenon are correctly anticipated when one admits the possibility of load induced residual stresses into his analysis. The potential importance of the $K_T\Delta S_1$-vs-σ analysis is only hinted at in Figs. 6 and 7. The potential lies in the possibility of developing a simple analysis technique than can be used to quantitatively explain sequence effects in notched components.

In accepting the idea of residual stresses, one also accepts the idea that residual stresses may be either life increasing or life decreasing depending on whether compressive or tensile residual stresses are induced. For instance, a component that normally is loaded in tension would experience an increased rate of fatigue damage if tensile residual stresses were induced in the structure. The same component loaded identically would enjoy a much longer lifetime if compressive residual stresses existed in the structure. Therefore, for the same maximum nominal stress level of a component one would expect longer lifetimes, lighter structures, and safer operation if detrimental residual stresses could be eliminated or minimized.

From Fig. 3 it is apparent that positive load peaks cause compressive residual stresses at notches provided the notch stress is higher than the material yield stress. In general, the higher the positive peak load the more compressive the residual stress at zero load. This residual stress serves to decrease the apparent stress level for spectrum loads below the previous positive peak load and thus one would expect an increased fatigue life. But, the greater the compressive residual stress the smaller the nominal compressive load necessary to cause significant compressive yielding and thus decrease, and perhaps change the sign of, the residual stress. Given a load spectrum that contains both tension and compression, one would have to assume that, at any time in a structural lifetime, residual stresses could exist that would be either detrimental or beneficial to the fatigue life. If a detrimental stress were known to have been introduced, one would reinstate beneficial stresses with a high tensile load. Because of the relative mobility of the residual stresses in a mixed tensile-compressive spectrum loading environment, it is doubtful whether a single cycle maximum preload of a structure would have any lasting beneficial effect on its life. A periodic positive overload of a structure would be necessary to show any increase in fatigue lifetime for a spectrum loaded vehicle.

A similar beneficial peak load residual stress type effect is the probable cause of crack propagation retardation in the fracture mechanics field. Broek and Schijve[17] show a factor of 5 increase in crack propagation lifetime due to the inclusion of positive peak loads in constant amplitude loading.

Safer and more reliable structures could be built if one could design the critical components so that only beneficial residual stresses could be produced. Such structures would be ones that experience only tensile loads or tensile with negligible compressive loads. Where beneficial residual stresses could not be designed into the system, increased lifetime could be obtained by controlling residual stresses on existing structures by causing periodic peak positive loads.

Summary

The existence of residual stresses and their potential effects in modifying structural fatigue lifetimes has been intuitively accepted by designer for many years. Generally, there has been little attempt, though, at transferring this residual stress awareness into aircraft design and operations probably because of the difficulty of developing a sufficiently accurate sequence dependent stress analysis.

There are two separate approaches that become apparent from an understanding of the Neuber analysis developed in this paper. The first involves the explicit use of the $K_T\Delta S_1$-vs-σ relationship to calculate the spectrum local stress amplitudes for use in the conventional cumulative damage analysis. The second involves the development of an aircraft design and operations philosophy based on an understanding of residual stresses. Potentially this analytic technique has the ability to bridge the gap between the conventional elastic and local residual stress analysis for the generally improved design of safe, fatigue resistant structures.

References

[1] Wetzel, R. M., "Smooth Specimen Simulation of the Fatigue Behavior of Notches," *Journal of Materials,* JMLSA, Vol. 3, No. 3, Sept. 1968, p. 646.

[2] Gowda, C. V. B. and Topper, T. H., "On the Relation Between Stress and Strain—Concentration Factors in Notched Members in Plane Stress," *Transaction of the ASME: Journal of Applied Mechanics,* Vol. 37, No. 1, March 1970.

[3] Crews, J. H., Jr., "Crack Initiation at Stress Concentrations as Influenced by Prior Local Plasticity," *Achievement of High Fatigue Resistance in Metals and Alloys, ASTM STP* **467**, American Society for Testing and Materials, 1970, pp. 37–52.

[4] Stadnick, S. J., *Simulation of Overload Effect in Fatigue Based on Neuber's Analysis*, Rept. 325, 1969, Dept. of Theoretical and Applied Mechanics, Univ. of Illinois, Urbana, Ill.

[5] Papirno, R., *Plastic Concentration Factors in Flat Notched Specimens of AISI* **4340** *Steel*, AMMRC TR 70-2, (AD 704 337), Feb. 1970, Army Materials and Mechanics Research Center, Watertown, Mass.

[6] Neuber, H., "Theory of Stress Concentration for Shear Strained Prismatical Bodies with Arbitrary Non Linear Stress Strain Law," *Transactions of the ASME: Journal of Applied Mechanics*, Dec. 1961, p. 544.

[7] Potter, J. M., *A General Fatigue Prediction Method Based on Neuber Notch Stresses and Strains*, AFFDL-TR-70-161 (AD 723 631), Feb. 1971, Air Force Flight Dynamics Lab., Wright-Patterson Air Force Base, Ohio.

[8] Crews, J. H., Jr., "*Local Plastic Stresses in Sheet Aluminium Alloy Specimens with Stress Concentration Factor of* **2** *Under Constant-Amplitude Loading*," TN D-3152, Dec. 1965, NASA.

[9] Crews, J. H., Jr., "*Elasto Plastic Stress-Strain Behavior at Notch Roots in Sheet Specimens Under wonstant-Amplitude Loading*," TN D-5253, June 1969, NASA.

[10] *Metallic Materials and Elements for Aerospace Vehicle Structures*, MIL-HDBK-5A, Feb. 1966, Dept. of Defense, Washington, D.C.

[11] Nauman, E. C., Hardrath, H. F., and Guthrie, D. E.,"Axial Load Fatigue Tests of 2024-T3 and 7075-T6 Aluminium Alloy Sheet Under Constant and Variable-Amplitude Loads," TN D-212, 1959, NASA.

[12] Illg, W., "Fatigue Tests on Notched and Unnotched Sheet Specimens of 2024-T4 and 7075-T6 Aluminium Alloy and of SAE 4130 Steel with Special Consideration to the Life Range from 2 to 10,000 Cycles," TN 3866, Dec. 1956, NASA.

[13] Breyan, W., "Effects of Block Size, Stress Level, and Loading Sequance on Fatigue Characteristics of Aluminium-Alloy Box Beams," *Effects of Environment and Complex Load History on Fatigue Life, ASTM STP* **462**, American Society for Testing and Materials, 1970, pp. 127–166.

[14] Raske, D. T., "The Variation of the Fatigue Notch Factor With Life," M. S. thesis, 1971, Dept. of Theoretical and Applied Mechanics, Univ. of Illinois, Urbana, Ill.

[15] Impellizzeri, L. F., "Cumulative Damage Analysis in Structural Fatigue," *Effects of Environment and Complex Load History on Fatigue Life, ASTM STP* **462**, American Society for Testing and Materials, 1970, pp. 40–68.

[16] Schijve, J., Broek, D., De Rijk, P., Nederveen, A., and Sevenhuysen, P. J., *Fatigue Tests with Random and Programmed Load Sequences, with and without Ground-To-Air Cycles. A Comparative Study on Full-Scale Wing wenter Sections*, AFFDL-TR-66-143, Oct. 1966, Air Force Flight Dynamics Lab., Wright-Patterson Air Force Base, Ohio.

[17] Broek, D., and Schijve, J., *The Influence of the Mean Stress on the Propogation of Fatigue Cracks in Aluminium Alloy Sheet*, NLR-TN M.2111, Jan. 1963, National Aero- and Astronautical Research Inst., Amsterdam.

OCTOBER 1972 AIAA JOURNAL VOL. 10, NO. 10

Free Vibration of Prestressed Cylindrical Shells Having Arbitrary Homogeneous Boundary Conditions

LESLIE E. PENZES*
Combustion Engineering Inc., Windsor, Conn.
AND
HARRY KRAUS†
Rensselaer Polytechnic Institute of Conn., Hartford, Conn.

An exact solution for the free vibration of orthotropic cylindrical shells having arbitrary boundary conditions is derived. The theory includes the combined effects of torsion, normal pressure, axial force, and rotation. The rotational effects contain the centrifugal and Coriolis forces. The mode shapes and the boundary determinant with torque effect, appear in complex form and cannot be reduced to real functions. The illustration of the coupled mode shapes is carried out in the form of a three-dimensional surface. The elimination of the torque reduces the displacement to real functions. Several numerical examples are given and they show excellent correlation with test results.

Nomenclature

ρ = mass density of the shell
h_s, h_b, h_m = orthotropic shell thickness associated with membrane, bending, and inertia effects of the shell
c_{ij}, s_{ij} = orthotropic elastic constants associated with membrane and bending effects
C^* = $(c_{11}c_{22} - c_{12}^2)$
u, v, w = displacements in the axial, tangential, and radial directions
t = time
Ω = rotational speed of shell
a = the mean radius of the cylindrical shell

Received December 6, 1971; revision received May 8, 1972. The results reported in this paper are taken from a Ph. D. thesis submitted by the first author to the Rensselaer Polytechnic Institute.

Index category: Structural Dynamic Analysis.

* Principal Engineer: formerly at Pratt & Whitney Aircraft, East Hartford, Conn. Member AIAA.

† Professor of Mechanics.

Introduction

ALTHOUGH many papers have been published on the free vibration of cylindrical shells, most of these studies are restricted to simply supported or clamped end conditions or the limited combinations of these with other restrictions. Forsberg presented an exact solution for free vibration of cylindrical shells with arbitrary homogeneous boundary conditions.[1] Smith and Haft considered the free vibrations of cylindrical shells with clamped boundary conditions.[2] Fung, Sechler, and Kaplan investigated the effects of internal pressure on the free vibration of cylindrical shells having simply supported boundary conditions.[3] Armenakas and Herrmann studied the vibrations of infinitely long cylindrical shells under the initial stresses due to uniform lateral and hydrostatic pressures, uniform bending moment, and radial shear.[4] The centrifugal and Coriolis forces are discussed by Macke assuming inextensional ring theory[5] and again by DiTaranto and Lessen including membrane effects of the infinitely long cylindrical shell.[6] Srinivasan and Lauterbach included the additional effect of torque to the membrane pre-